01 Oct 2007

Prediction of the Kolmogorov Entropy Derived from Computed Tomography Data in a Bubble Column Operated under the Transition Regime and Ambient Pressure

Stoyan Nedeltchev

Ashfaq Shaikh

Muthanna H. Al-Dahhan
Missouri University of Science and Technology, aldahhanm@mst.edu

Recommended Citation

S. Nedeltchev et al., "Prediction of the Kolmogorov Entropy Derived from Computed Tomography Data in a Bubble Column Operated under the Transition Regime and Ambient Pressure," *Chemical Engineering and Technology*, vol. 30, no. 10, pp. 1445 - 1450, Wiley; Gesellschaft Deutscher Chemiker; Gesellschaft für Chemische Technik und Biotechnologie, Oct 2007.
The definitive version is available at https://doi.org/10.1002/ceat.200700053

Stoyan Nedeltchev[1]
Ashfaq Shaikh[2,3]
Muthanna Al-Dahhan[2]

[1] Institute of Chemical Engineering, Bulgarian Academy of Sciences, Bulgaria.

[2] Department of Chemical Engineering, Washington University in St. Louis, Chemical Reaction Engineering Laboratory, MO, USA.

[3] Present address: Global PET Intermediates Technology, Eastman Chemical Company, Kingsport, TN, USA.

Communication

Prediction of The Kolmogorov Entropy Derived from Computed Tomography Data in a Bubble Column Operated under The Transition Regime and Ambient Pressure

The Kolmogorov entropy (KE) algorithm was successfully applied to single source γ-ray Computed Tomography (CT) data measured by three scintillation detectors in a 0.162 m-ID bubble column equipped with a perforated plate distributor (163 holes × ∅ $1.32 \cdot 10^{-3}$ m). The aerated liquid height was set at 1.8 m. Dried air was used as a gas phase, while Therminol LT (ρ_L = 886 kg m^{-3}, μ_L = $0.88 \cdot 10^{-3}$ Pa s, $\sigma = 17 \cdot 10^{-3}$ N m^{-1}) was used as a liquid phase. At ambient pressure, the superficial gas velocity, u_G, was increased stepwise with an increment of 0.01 m s^{-1} up to 0.2 m s^{-1}. Based on the sudden changes in the KE values, the boundaries of the following five regimes were successfully identified: dispersed bubble regime ($u_G < 0.02$ m s^{-1}), first transition regime ($0.02 \le u_G < 0.08$ m s^{-1}), second transition regime ($0.08 \le u_G < 0.1$ m s^{-1}), coalesced bubble regime consisting of four regions (called 4-region flow; $0.1 \le u_G < 0.12$ m s^{-1}), and coalesced bubble regime consisting of three regions (called 3-region flow; $u_G > 0.12$ m s^{-1}). The KE values derived from three scintillation detectors in the first transition regime were successfully correlated to both bubble frequency and bubble impact. The latter was found to be inversely proportional to the bubble Froude number. The KE model implies that the bubble size in this particular flow regime is a weak function of the orifice Reynolds number ($d_b = 7.1 \cdot 10^{-3} \mathrm{Re}_0^{-0.05}$).

Keywords: Bubble column, Computed Tomography, Kolmogorov entropy, Transition regime

Received: February 11, 2007; *revised:* May 22, 2007; *accepted:* July 02, 2007

DOI: 10.1002/ceat.200700053

1 Introduction

Numerous industrial gas-liquid reactions (hydrogenation, oxidation, chlorination, alkylation, aerobic fermentation, ozonolysis, coal liquefaction, etc.) are performed in bubble columns [1, 2]. Bubble columns are finding increasing application in the processes for converting natural gas to liquid fuels (Fischer-Tropsch synthesis) as well as waste water treatment and methanol synthesis. In these chemical reactors, gas is dispersed in the form of bubbles in a pool of liquid through a gas distributor or sparger.

The flow regime diagnostics is necessary for a reliable modeling, design, and control of bubble columns. Nedeltchev et al. [3] found that the bubble column exhibits a complex behavior which passes through five different flow regimes: dispersed bubble ($u_G < 0.02$ m s^{-1}), first transition ($0.02 \le u_G < 0.08$ m s^{-1}), second transition ($0.08 \le u_G < 0.1$ m s^{-1}), coalesced bubble (4-region flow; $0.1 \le u_G < 0.12$ m s^{-1}) and coalesced bubble (3-region flow; $u_G > 0.12$ m s^{-1})[1)]. The existence of all these regimes has already been documented by Chen et al. [4], Lin et al. [5], Olmos et al. [6, 7], and Barghi et al. [8]. The boundaries of the different flow regimes have been identified based on the sudden changes in the values of both KE and average absolute deviation [3, 9]. Earlier, Shaikh and Al-Dahhan [10] identified the transition point between homogeneous and heterogeneous flow regimes based on the analysis of the steepness of the gas holdup radial profile measured by means of Computed Tomography (CT). These authors have summarized well the other intrusive techniques for flow regime identification.

Correspondence: Dr. S. Nedeltchev (snn13@gmx.net), Institute of Chemical Engineering, Bulgarian Academy of Sciences, Acad. G. Bontchev Str. Bl. 103, 1113 Sofia, Bulgaria.

1) List of symbols at the end of the paper.

The various flow regime transitions depend largely on reactor geometry, gas distribution, and physico-chemical properties of the two phases. The design of bubble columns involves a precise determination of the operating flow regime. Some new techniques such as wavelet analysis, artificial neural networks, and chaos analysis must be applied more rigorously for flow regime identification and scale-up of bubble columns.

Nonlinear chaos theory is a very promising method for the investigation of multiphase flow behavior in bubble columns. Many experimental findings have shown that chaos analysis can be used for the quantitative characterization of the hydrodynamic behavior and flow regime transitions in bubble columns. Chaos analysis involves the state space analysis, which has demonstrated its usefulness for extracting the dynamic information hidden within the time series [11]. A more detailed knowledge of the chaotic behavior of bubble columns can lead to better design and operation with resultant improvement in performance.

Devanathan et al. [12] revealed that the flow in bubble columns is transient and chaotic even at low superficial gas velocities, u_G. The dynamics of a chaotic system is characterized by its attractor. The chaotic attractor maintains its embedding dimension, i.e. it has structure. The essential characteristic of a chaotic attractor is sensitivity to initial conditions. Thus any two initial points, no matter how close together, will grow apart exponentially in time. The complexity of the reconstructed attractor can be evaluated analytically with the correlation dimension and the Kolmogorov entropy (KE). The former is theoretically related to the degrees of freedom of the system, while the latter indicates the rate of information loss with time evolution in the system.

Over the past two decades, many researchers have applied the nonlinear chaos analysis to bubble column reactors. For instance, chaos analysis was applied to gas holdup fluctuations [9], pressure fluctuation time series [13–17], Computer-Automated Radioactive Particle Tracking (CARPT) data [18, 19], bubbling frequency [20], etc. All of these studies demonstrated that the chaos methodology can provide us with important insights into the complex hydrodynamics of gas-liquid bubble columns.

A chaotic system is a nonlinear system that is extremely sensitive to small changes in initial conditions. Two initial states of the system that are almost identical will, after some time, develop in completely different ways. The rate at which these differences grow is expressed in quantities like Lyapunov exponents and Kolmogorov entropy (KE), which quantify the degree of unpredictability of the system. It has been found that the KE is an extremely useful parameter to quantify the "degree of chaos" which bubble columns apparently exhibit. The KE is a quantitative measure of the amount of information which is lost or gained by a system as it evolves. This chaotic parameter can be considered as a measure of the degree of predictability of a time series. It is used to compute the invariant properties of the corresponding attractor. The prediction of KE is useful to characterize the dynamic behavior of bubble columns.

Positive and finite KE is a sufficient condition for chaos and the chaotic system is only to some extent predictable over a restricted time interval. The dynamics of the chaotic system are fully represented by the so-called strange attractor in the phase space. The strange attractor is a very complicated geometric figure which is characterized by a noninteger dimension. The attractor of the chaotic system is not finite and the system never returns to the same state. The KE can be used conveniently to characterize the reconstructed attractors.

In our previous paper [3], we estimated the degree of chaos in the bubble column by means of the KE algorithm [21] applied to Computed Tomography (CT) data. The KE is considered as a measure of the rate of loss of information in the system (expressed in bits of information per second). In other words, KE quantifies the degree of unpredictability of the system. This parameter is sensitive to changes in operating conditions and that is why we employed it for the sake of flow regime identification. In the KE algorithm [21], the KE was calculated from the average number of steps required for a pair of vectors, which are initially within a specific maximum length to separate until the distance between the pair becomes larger than the specific maximum length. For all the pairs of points on the attractor, the number of steps were calculated and then the average number was estimated.

In this communication, it will be demonstrated that the KE values in the first transition regime can be predicted by means of a theoretical model. The KE algorithm [21] was applied to the time series measured simultaneously by three scintillation detectors at ambient pressure. As in our previous paper [3], the key parameters in the KE algorithm were set as follows: 10000 points obtained at a sampling frequency of 20 Hz, embedding dimension equal to 50, time delay equal to unity and cut-off length set equal to three times the average absolute deviation of the experimental data. In addition, it will be explained how the KE values derived from both CARPT and CT data can be compared in the transition regime and how a dimensionless KE number can be defined and held constant.

2 Experimental

The CT experiments were performed in a 0.162 m-ID stainless steel column with a total height of 2.5 m. The column was equipped with a perforated plate distributor (163 holes × ∅ $1.32 \cdot 10^{-3}$ m, 1.09 % open area). The aerated liquid height was kept constant at 1.8 m. The schematics of the setup and the experimental details are presented elsewhere [10]. The data used in this study for KE analysis was obtained in flow regime studies via CT by Shaikh and Al-Dahhan [10].

Air was used as the gas phase, while Therminol LT (μ_L = $0.88 \cdot 10^{-3}$ Pa s, ρ_L = 886 kg m^{-3}, $\sigma = 17 \cdot 10^{-3}$ N m^{-1}) was used as the liquid phase. The u_G values were varied from 0.01 to 0.2 m s^{-1} with an interval of 0.01 m s^{-1}. The present work is based on CT data obtained only at ambient pressure. Software and hardware details of the single source γ-ray CT are explained elsewhere [22]. The CT scanner is a versatile instrument that enables the quantification of the time-averaged holdup distribution for two-phase flows under a wide range of operating conditions. The CT setup consists of an array of scintillation detectors with an opposing source, which rotate together around the object to be scanned. The CT scanner uses a Cesium (Cs-137) encapsulated γ-ray source with an activity

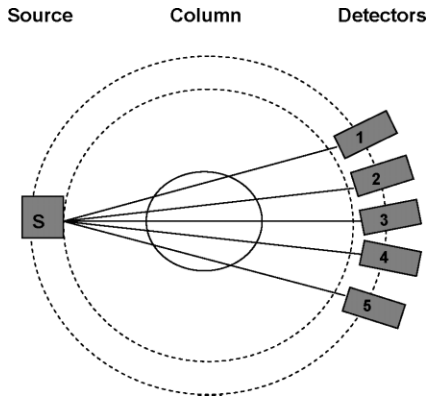

Figure 1. Schematics of the five strategically located scintillation detectors. An encapsulated γ-ray source (Cs-137) is installed opposite the detectors. CT scans were taken at an axial height of 0.89 m.

of ~85 mCi. The array of detectors and the source are mounted on a gantry which can be rotated 360° around the object to be scanned, using a stepper motor interfaced to a host computer. In addition, the source-detector setup can be moved up and down to scan cross-sections at any axial position of the column. Each detector consists of a cylindrical 0.051×0.051 m NaI crystal, a photo multiplicator and electronics, forming a 0.054×0.26 m cylindrical assembly. In each view, each detector acquires 7 projections covering the total angular span of 2.72° of the detector face. The position of each scintillation detector is given in Fig. 1.

A total of 99 views were acquired, with 3.6° in angular shift after every view. Hence, 3465 ($5 \times 7 \times 99$) projections were used to reconstruct the phase holdup distribution at each cross-sectional plane. All CT scans were performed at an axial height of 0.89 m (at this elevation, end effects are negligible). The CT data was originally obtained using five scintillation detectors [10]. However in this work, the results obtained from only three of them (first, second, and fourth) are presented. In the current work, the raw photon counts obtained using detectors at various views and projections were combined to form a time series corresponding to that particular detector. This time series was utilized for KE analysis. Further details about the CT experimental facility can be found in Rados [23] and Rados et al. [24].

3 Results and Discussion

In our recent paper [3] we successfully identified by means of the KE algorithm [21], the boundaries of the following five flow regimes: dispersed bubble ($u_G < 0.02$ m s^{-1}), first transition ($0.02 \le u_G < 0.08$ m s^{-1}), second transition ($0.08 \le u_G < 0.1$ m s^{-1}), coalesced bubble (4-region flow; $0.1 \le u_G < 0.12$ m s^{-1}) and coalesced bubble (3-region flow; $u_G > 0.12$ m s^{-1}). The KE values were derived from CT data taken by the first (detector No. 1 in Fig. 1) scintillation detector. These results are presented in Fig. 2.

In addition, the KE values derived from the readings of the second scintillation detector are also presented (see Fig. 3). The same trends and transitional gas velocities are observed.

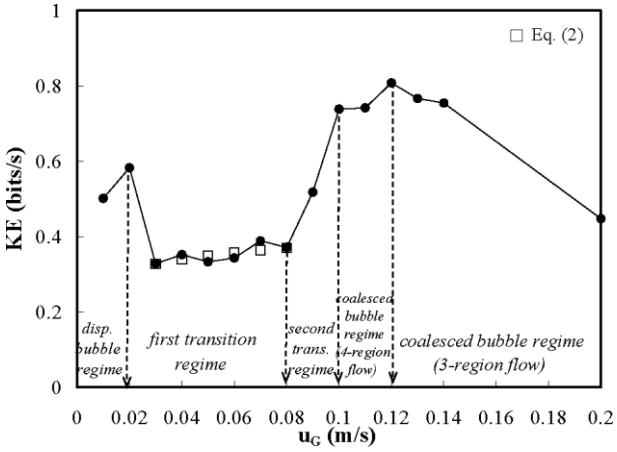

Figure 2. Kolmogorov entropy (KE) values derived from the readings of the first scintillation detector as a function of the superficial gas velocity, u_G.

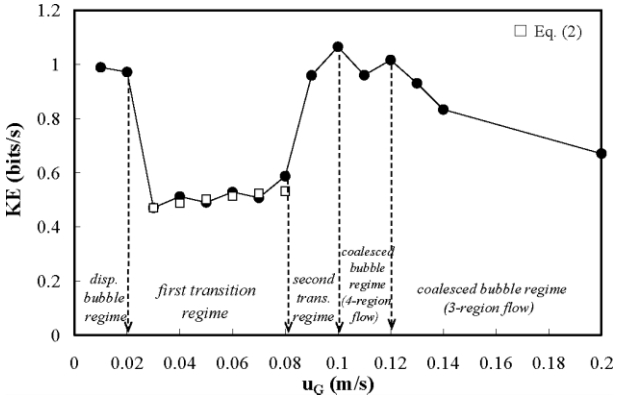

Figure 3. Kolmogorov entropy (KE) values derived from the readings of the second scintillation detector as a function of the superficial gas velocity, u_G.

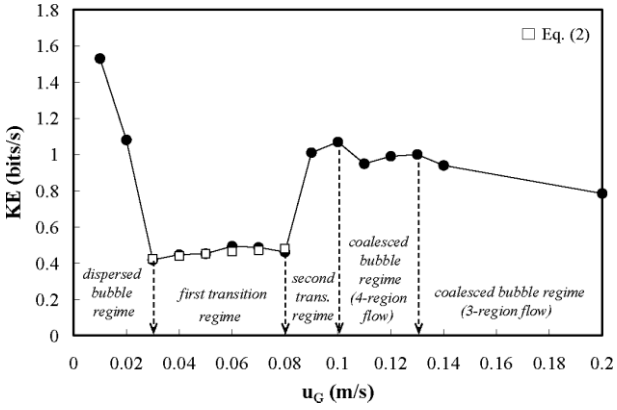

Figure 4. Kolmogorov entropy (KE) values derived from the readings of the fourth scintillation detector as a function of the superficial gas velocity, u_G.

Fig. 4 exhibits the KE values derived from the readings of the fourth scintillation detector. As these KE results are compared with the KEs derived from the first (see Fig. 2) and second (see Fig. 3) detectors, it turns out that the first (0.03 m s^{-1}) and the fourth (0.13 m s^{-1}) transition velocities are somewhat delayed.

It is obvious that the boundaries of the different flow regimes identified by means of the KE algorithm [21] applied to the readings of the first, second, and fourth scintillation detectors practically coincide. In other words, the sudden changes in the KE values occur at approximately the same u_G values. It is worth noting that the KE values derived from the second and fourth scintillation detectors are somewhat higher.

Especially interesting is the first transition regime since the obtained KE values enable us to establish a theoretical model for prediction of the KE values falling into this particular hydrodynamic regime. The transition regime is characterized by large flow macrostructures (large eddies) and widened bubble size distribution due to the onset of bubble coalescence [6, 7]. This regime corresponds to the development of local liquid circulation patterns in the column. It is well established that the occurrence and the persistence of the transition regime depends largely on the uniformity and the quality of the aeration. In the first transition regime, the large bubbles are formed only in the distributor region. Olmos et al. [6] argue that the flow structure is not well established in the first transition regime. Bubble coalescence only occurs near the gas sparger. The central bubble plume is unstable and beyond a certain liquid height, the flow structure returns to that existing in the dispersed bubble regime with individual trajectories. Olmos et al. [7] argue that in the first transition regime, the established flow pattern is still homogeneous despite some predominating bubble paths in the column center. In the vicinity of the gas distributor, the flow structures evolve and liquid macrostructures occur.

3.1 Kolmogorov Entropy (KE) Prediction in The First Transition Regime

The theoretical prediction of the KE in the field of bubble columns is a new and challenging area. This chaotic parameter takes different values under the different flow regimes and this fact should be taken into account in every theoretical model. Nedeltchev et al. [19] developed models for the prediction of the KE values derived from CARPT data obtained in both bubbly and transition flow regimes. Nedeltchev [25] modeled the KE values derived from pressure fluctuations measured under the fully developed churn-turbulent regime. The KE modeling is an important step for bubble column scale-up based on the chaos methodology.

The KE calculations are very time-consuming. It is worth noting that KE takes part in a dimensionless scale-up criterion called a chaotic similarity group [11, 25]. The latter should be kept constant in the case of a proper dimensionless scaling. In other words, both lab-scale and industrial-scale units should have the same "degree of unpredictability", i.e. they should lose their information in a similar way. Hence, we sought to develop a correlation for the KE prediction, which will be helpful towards the scale-up of these gas-liquid reactors. The KE values in the first transition regime can be predicted successfully by means of the following model:

$$KE = C(bubble\ frequency)(bubble\ impact) = C\frac{Q_G}{V_B}Fr_B^{-1}$$

$$= C\frac{(\pi D_c^2/4)u_G}{(\pi d_b^3/6)}\frac{(gd_b)^{0.5}}{u_G} \quad (1)$$

It is worth noting that Nedeltchev and coworkers [19, 25] and van den Bleek et al. [26] also correlated the KE to both bubble frequency and bubble impact. The bubble Froude number, Fr_B, characterizes the ratio of inertial to gravity forces at the bubble scale. The bubble impact should be taken into account in the KE model since the bubbles are the major cause of the complexity in bubble columns.

The elimination of all the repeated terms yields:

$$KE = 4.698C\frac{D_c^2}{d_b^{2.5}} \quad (2)$$

It is clear from Eq. (2) that the prediction of KE needs an estimation of bubble diameter, d_b. The four main correlations (see Tab. 1) that are available in the literature were tested for an estimation of bubble diameter. The most suitable correlation for estimation of bubble diameter was selected based on a comparison between the predicted and experimental KEs in the first transition regime. Tab. 1 lists the proportionality constant, average relative error (ARE), and maximum relative error (MRE) when the KE values (measured by first, second, and fourth scintillation detectors) are predicted by means of four different correlations for bubble size estimation. Using the nonlinear regressional analysis, the proportionality constants, C, for the first, second, and fourth scintilation detectors were determined.

Fig. 5 shows the parity plot between experimental and calculated KEs using the four different correlations for bubble size estimation which are given in Tab. 1. It is clear from Tab. 1 and Fig. 5 that the prediction of the KE in the first transition regime using the bubble size correlation of Bhavaraju et

Table 1. Statistical comparison of KE predictions based on four different correlations for bubble size estimation.

Correlations for bubble size	I detector	II detector	IV detector
Bhavaraju et al. [27]	$C = 5.71 \cdot 10^{-6}$ ARE = 3.19 % MRE = 6.31 %	$C = 8.2 \cdot 10^{-6}$ ARE = 3.77 % MRE = 9.45 %	$C = 7.4 \cdot 10^{-6}$ ARE = 2.76 % MRE = 6.15 %
Akita and Yoshida [28]	$C = 1.16 \cdot 10^{-6}$ ARE = 5.89 % MRE = 12.81 %	$C = 1.75 \cdot 10^{-6}$ ARE = 5.07 % MRE = 9.17 %	$C = 1.58 \cdot 10^{-6}$ ARE = 5.2 % MRE = 12.83 %
Wilkinson et al. [29]	$C = 1.18 \cdot 10^{-6}$ ARE = 4.17 % MRE = 11.05 %	$C = 1.73 \cdot 10^{-6}$ ARE = 4.42 % MRE = 13.04 %	$C = 1.57 \cdot 10^{-6}$ ARE = 3.25 % MRE = 7.79 %
Pohorecki et al. [30]	$C = 6.77 \cdot 10^{-7}$ ARE = 6.06 % MRE = 13.24 %	$C = 1.02 \cdot 10^{-6}$ ARE = 5.19 % MRE = 9.33 %	$C = 9.06 \cdot 10^{-7}$ ARE = 5.86 % MRE = 11.68 %

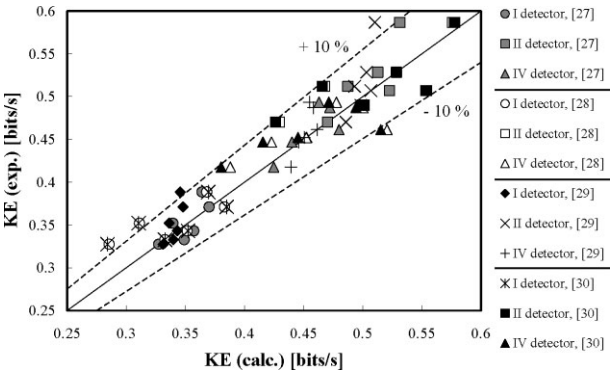

Figure 5. Parity plot of the Kolmogorov entropies (KE) in the first transition regime derived from three different scintilation detectors. The bubble size was calculated using four different correlations [27–30].

al. [27] statistically outperforms the ones using the other selected correlations. Bhavaraju et al. [27] reported that the mean bubble diameter, d_b, can be estimated as follows:

$$d_b = 7.1 \cdot 10^{-3}\,\mathrm{Re}_0^{-0.05} = 7.1 \cdot 10^{-3}\left(\frac{4Q_G\rho_G}{\pi N_h d_0 \mu_G}\right)^{-0.05} \quad (3)$$

where N_h is the number of distributor holes and d_0 is the size of the hole.

Within the boundaries ($0.03 \le u_G \le 0.08$ m s^{-1}) of the first transition regime, the bubble size, d_b, (calculated by means of Eq. (3)) decreases in the range of $5.41–5.15 \cdot 10^{-3}$ m. It was found that using Eq. (3), the theoretical KE values are closest to the experimental ones. The predicted KEs by means of Eqs. (1–3) are also exhibited in Figs. 2–4 (see the open squares).

3.2 Adjusting The Same Dimensionless KE Numbers between Two Different Gas-Liquid Systems Operated in The Transition Regime

Nedeltchev et al. [19] modeled the KE values derived from CARPT data in an air-water system operated in the transition regime. It is worth noting that the bubble size was also estimated by means of Eq. (3). The column had the same inner diameter (0.162 m) and was equipped with a perforated plate gas distributor (82 holes × ∅ $0.4 \cdot 10^{-3}$ m). The sampling frequency was set at 50 Hz. The same number of points (10000), embedding dimension (50), and time delay (unity) were used.

At u_G = 0.09 m s^{-1}, Nedeltchev et al. [19] reported that KE (derived from CARPT) is equal to 1.451 bits s^{-1}. This value should be converted into a dimensionless KE number. According to the maximum-likelihood estimator [21], KE is directly proportional to the sampling frequency. Therefore, the KE value expressed in bits·s^{-1} should be divided by the sampling frequency in order to obtain a dimensionless KE number. In the aforementioned case, the dimensionless KE number is equal to 0.029 (1.451/50).

If the same dimensionless KE number can be obtained in any other gas-liquid system, then both dispersions will be characterized with the same degree of chaos, i.e. the same flow patterns will be established. In other words, both gas-liquid systems will lose information in a similar way. Fig. 3 shows that at u_G = 0.08 m s^{-1}, the photon counts from the second scintillation detector yield KE = 0.587 bits s^{-1}. It is worth noting that this KE value is very close to the value of 0.563 bits s^{-1} derived from the third scintillation detector at the same operating condition (see Fig. 4). The sampling frequency during all CT runs was set at 20 Hz. Thus, the dimensionless KE number is again equal to 0.029 (0.587/20). From a chaotic viewpoint, this means that the behavior of both gas-liquid systems (air-water and air-Therminol LT) at these particular operating conditions are characterized with the same degree of predictability (complete chaotic similarity). This state is called conservation of information. In the air-water system, the bubble size at u_G = 0.09 m s^{-1} is equal to $4.66 \cdot 10^{-3}$ m (Eq. (3)), whereas in the air-Therminol LT system, the bubble size at u_G = 0.08 m s^{-1} is equal to $5.15 \cdot 10^{-3}$ m (Eq. (3)). We see that not only the dimensionless KE numbers are equal but also the gas velocities, u_G, and bubble sizes, d_b, are close. The KE-based flow regime identifications [3, 19] reveal that both conditions fall in the transition flow regime. Hence, maintaining the same dimensionless KE number will assure the same flow pattern in both gas-liquid systems. The KE prediction is an important step in the process of matching the dimensionless KE numbers since it gives us a possibility to control the KE and also provides an indirect way to suggest the suitable bubble size correlation applicable in the first transition regime.

The example presented above demonstrates that the KE values obtained using advanced gamma ray-based techniques such as CARPT and CT are comparable regardless of the sampling frequency.

4 Conclusion

The boundaries of five flow regimes have been identified by means of the KE algorithm applied to Computed Tomography (CT) data, taken by three different scintillation detectors. A theoretical approach for the KE prediction in the first transition regime was developed. It was found that the KE values can be correlated successfully to both bubble frequency and bubble impact. The latter is inversely proportional to the bubble Froude number. The KE model was verified by the experimental data of three different scintillation detectors. It was found that this theoretical approach can be applied successfully in the first transition regime instead of the time-consuming KE calculations based on long experimental time series. By means of a real example, the importance of the KE modeling as well as maintaining the same dimensionless KE number in two different gas-liquid systems were demonstrated.

Acknowledgement

Dr. Stoyan Nedeltchev expresses his gratitude to the Bulgarian-American Fulbright Commission for the research grant provided. Dr. Ashfaq Shaikh and Prof. Muthanna Al-Dahhan are thankful to the High Pressure Slurry Bubble Column Reactor (HPSBCR) Consortium [Conoco-Philips (USA), Eni Tech

(Italy), Sasol (South Africa), Statoil (Norway)] and UCR-DOE (DE-FG-26-99FT40594) grants that made the experimental work possible.

Symbols used

C	[–]	proportionality constant
d_0	[m]	orifice diameter
d_b	[m]	bubble size
D_c	[m]	column diameter
g	[m s^{-2}]	acceleration due to gravity
KE	[bits s^{-1}]	Kolmogorov entropy
N_h	[–]	number of distributor holes
Q_G	[m^3 s^{-1}]	gas flow rate
u_G	[m s^{-1}]	superficial gas velocity
V_B	[m^3]	bubble volume

Greek symbols

μ_G	[Pa s]	gas viscosity
ρ_G	[kg m^{-3}]	gas density
μ_L	[Pa s]	liquid viscosity
ρ_L	[kg m^{-3}]	liquid density
σ	[N m^{-1}]	liquid surface tension

Dimensionless numbers

Re_0	[–]	orifice Reynolds number
Fr_B	[–]	bubble Froude number

References

[1] W.-D. Deckwer, *Bubble Column Reactors*, John Wiley, New York **1992**.
[2] L.-S. Fan, *Gas-Liquid-Solid Fluidization Engineering*, Butterworth, Stoneham, MA **1989**.
[3] S. Nedeltchev, A. Shaikh, M. Al-Dahhan, *Chem. Eng. Tech.* **2006**, *29 (9)*, 1054. DOI: 10.1002/ceat.200600162
[4] R. C. Chen, J. Reese, L.-S. Fan, *AIChE J.* **1994**, *40*, 1093.
[5] T.-J. Lin, J. Reese, T. Hong, L.-S. Fan, *AIChE J.* **1996**, *42*, 301.
[6] E. Olmos, C. Gentric, S. Poncin, N. Midoux, *Chem. Eng. Sci.* **2003**, *58*, 1731.
[7] E. Olmos, C. Gentric, N. Midoux, *Can. J. Chem. Eng.* **2003**, *81*, 382.
[8] S. Barghi, A. Prakash, A. Margaritis, M. A. Bergougnou, *Can. J. Chem. Eng.* **2004**, *82*, 865.
[9] S. Nedeltchev, U. Jordan, O. Lorenz, A. Schumpe, *Chem. Eng. Tech.* **2007**, *30 (4)*, 534. DOI: 10.1002/ceat.200600344
[10] A. Shaikh, M. Al-Dahhan, *Flow Meas. Instrum.* **2005**, *16*, 91.
[11] C. M. van den Bleek, J. C. Schouten, *Chem. Eng. Sci.* **1993**, *48*, 2367.
[12] N. Devanathan, M. P. Dudukovic, A. Lapin, A. Lübbert, *Chem. Eng. Sci.* **1995**, *50*, 2661.
[13] H. M. Letzel, J. C. Schouten, R. Krishna, C. M. van den Bleek, *Chem. Eng. Sci.* **1997**, *52*, 4447.
[14] V. V. Ranade, R. P. Utikar, *Chem. Eng. Sci.* **1999**, *54*, 5237.
[15] Y. Kang et al., *Chem. Eng. Sci.* **2000**, *55*, 411.
[16] T.-J. Lin, R.-C. Juang, Y.-C. Chen, C.-C. Chen, *Chem. Eng. Sci.* **2001**, *56*, 1057.
[17] T.-J. Lin, R.-C. Juang, C.-C. Chen, *Chem. Eng. Sci.* **2001**, *56*, 6241.
[18] M. Cassanello et al., *Chem. Eng. Sci.* **2001**, *56*, 6125.
[19] S. Nedeltchev, S. Kumar, M. P. Dudukovic, *Can. J. Chem. Eng.* **2003**, *81*, 367.
[20] R. Kikuchi et al., *Chem. Eng. Sci.* **1997**, *52*, 3741.
[21] J. C. Schouten, F. Takens, C. M. van den Bleek, *Phys. Rev. E* **1994**, *49*, 126.
[22] S. B. Kumar, *D. Sc. Thesis*, Washington University, St. Louis, MO **1994**.
[23] N. Rados, *D. Sc. Thesis*, Washington University, St. Louis, MO **2003**.
[24] N. Rados, A. Shaikh, M. H. Al-Dahhan, *Chem. Eng. Sci.* **2005**, *60*, 6067.
[25] S. Nedeltchev, *Bulg. Chem. Ind.* **1998**, *69*, 35.
[26] C. M. van den Bleek, M.-O. Coppens, J. C. Schouten, *Chem. Eng. Sci.* **2002**, *57*, 4763.
[27] S. M. Bhavaraju, T. W. F. Russell, H. W. Blanch, *AIChE J.* **1978**, *24*, 454.
[28] K. Akita, F. Yoshida, *Ind. Eng. Chem., Proc. Des. Dev.* **1974**, *13*, 84.
[29] P. M. Wilkinson, H. Haringa, L. L. van Dierendonck, *Chem. Eng. Sci.* **1994**, *49*, 1417.
[30] G. Pohorecki et al., *Chem. Eng. J.* **2005**, *113*, 35.

